Available online at www.sciencedirect.com
ScienceDirect
Ceramics International 35 (2009) 1855–1861
CERAMICS INTERNATIONAL
www.elsevier.com/locate/ceramint

Electrophoretic shaping of sub-micron alumina in ethanol☆

Meng Shan [a,b], Xiaojian Mao [a,b], Jian Zhang [a], Shiwei Wang [a,*]

[a] Shanghai Institute of Ceramics, Chinese Academy of Sciences, 1295 Dingxi Road, Shanghai 200050, PR China
[b] Graduate School of Chinese Academy of Science, Beijing 100039, PR China

Received 14 January 2008; received in revised form 30 May 2008; accepted 12 October 2008
Available online 25 November 2008

Abstract

The electrophoretic deposition (EPD) method was used to shape sub-micron Al_2O_3 green body in ethanol. The uniformity of the final deposit was affected by the colloidal properties of the suspension. Therefore, the stability of Al_2O_3 suspension in ethanol was studied in terms of electrophoretic mobility, viscosity and conductivity. The EPD kinetics were further investigated with different electrical conditions. The effect of cellulose acetate membrane on deposit was also studied. The green body with a relative density of about 60 %TD was associated with a narrow pore size distribution, indicating a high homogeneity of particle coordination. After presintering and HIPing at 1250 °C, a fully dense alumina ceramic was obtained with an average grain size of 0.65 μm.

Keywords: D. Al_2O_3; Sub-micron; Membrane method; Electrophoretic deposition

1. Introduction

It is known that translucent Al_2O_3 ceramics are widely used as the key components for high pressure sodium lamp and semiconductor-making device, which are sintered at very high temperatures (>1700 °C) for a long time, resulting in coarse grains (>15 μm), low hardness (~18 GPa) and limited strength (~300 MPa) [1,2]. Recently, remarkable progress has been made in producing fully dense sub-micron (<0.7 μm) alumina (porosity <0.05%) with excellent optical properties and mechanical properties (HV10 ≥20 GPa and 650–850 MPa in three-point bending) [3–5]. For this purpose, ultrafine (e.g. D_{50} = 150 nm) powders with high purity are required [6]. However, the potential advantages of very fine-grained powders are opposed by difficulties in shaping when a green body with a most homogeneous arrangement of powders on a microscale is the key to reach closed porosity (>95 %TD) at much lower presintering temperatures (<1300 °C), which is a prerequisite for hot isostatic pressing (HIP, <1300 °C) to sufficiently eliminate residual pores with suppressed grain growth in the present investigation [7,8]. However, conventional cold isostatic pressing (CIP) of granulated ultrafine powders is frequently ineffective to associate a higher density of green bodies >55 %TD with an optimized microstructural homogeneity because the external force can never arrive on an individual particle in the body to shift it into an optimum position between its neighbors [7,8]. On the contrary, wet shaping processes (e.g. gel casting, slip casting) can provide the freedom for particles to find this position on their own, exhibiting a generally improved homogeneity with a smaller total width of the distribution and a steeper slope at the center of the pore size distribution than CIP [7,8]. Therefore, casting approaches are applicable for obtaining transparent alumina [3,7]. However, they always involve several kinds of additives and high concentration of additives, which will cause a great quantity of harmful gases.

Electrophoretic deposition (EPD), a convenient electrochemical shaping technique, combining the advantages of the colloidal processing and the electric field assisted processing of ceramics [9], has attracted increasing interests due to its great potential on producing bulk ceramic materials [10–13] with three important advantages of versatility, low cost and reliability. A necessary condition for reaching a dense and homogeneous particle packing in the deposits, is well-dispersed, stable suspensions. The suspension stabilization

☆ Supported by the National High Technology Research and Development Program of China (No. 2006AA03Z535).
* Corresponding author. Tel.: +86 21 52414320; fax: +86 21 52413903.
E-mail address: swwang51@mail.sic.ac.cn (S. Wang).

0272-8842/$34.00
doi:10.1016/j.ceramint.2008.10.033

can be realized by (i) electrostatic repulsion between particles; (ii) steric interactions of molecules adsorbed on the surface of the particles; (iii) electrosteric stabilization, a combination of the other two methods. Simultaneously, the electrophoretic mobility has to be sufficiently high. To comply with these requirements, a suitable pH value is adjusted and/or organic additives are added.

EPD can be preformed in aqueous and non-aqueous suspensions, each of them having advantages and disadvantages. Water is used as a solvent for EPD mainly because of environmental and economical reasons. However, due to the electrolysis of water and the concomitant formation of gas bubbles at the electrodes, special methods are necessary to prevent macropores in the deposits, such as the use of cathode materials which can store hydrogen within their structure (e.g. palladium) [14,15] or the so-called membrane method described in Ref. [16]. In the case of this method, the EPD cell is subdividing into two compartments with an ion-permeable membrane, and the particles are deposited at the membrane. Recently, Braun et al. [17] have successfully prepared transparent Al_2O_3 ceramics by means of EPD from aqueous suspensions, using this membrane method. Contrarily, the particles could be deposited directly at the electrode in non-aqueous suspensions because the problems arising from the electrolysis of water can be avoided, and then the EPD cell requires no further processing. Besides, higher deposition rates can be obtained in non-aqueous suspensions by applying high voltages. Furthermore, in aqueous suspensions, additional factors influencing the EPD kinetics and the formation of the deposit have to be kept in mind [16], such as the ratio of the electrical conductivities of the liquid in the electrolyte compartment and of the suspensions. And Joule heating is greatly reduced in non-aqueous suspensions because of its smaller electrical conductivities [18]. Among the non-aqueous media, ethanol is the common dispersing medium for EPD.

Note that the particles in suspension will move only in response to the electric field if they carry a charge. However, the low dielectric constants of organic liquids limit the dissociation of surface groups, and additional mechanisms must be suggested to understand the charge developed on suspended alumina particles. The mechanism of charging in ethanol, a protic organic liquid, should be similar to water, i.e., proton transfer. It is based on the particle (M) in solvent (S) functioning as a proton donor or acceptor. The sign of the charge will depend on the direction of the transfer [19], i.e.:

$$MH_2^+ + S^- \rightleftharpoons MH + SH \rightleftharpoons M^- + SH_2^+$$

where MH and SH are the surface group on the particle and the solvent molecule, respectively. And the relative acid–base character of the solid surface and the liquid determines the sign of the charge. Moreover, the residual water in ethanol tends to adsorb at the particle/solvent interfaces, thus rendering the particles more basic [19]. The amphoteric surface sites on Al_2O_3 (AlOH) act as basic sites relative to ethanol because of the adsorption of water, resulting in the positively charged surface. And there is an acidity-dependent surface charge on Al_2O_3 suspended in ethanol. The charging mechanism of the surface was explained by adsorption of protons or hydroxyl groups on the Al_2O_3 surface as potential-determining ions following the reaction [20]:

$$AlOH_2^+ \xleftarrow{H^+} AlOH \xrightarrow{OH^-} AlO^- + H_2O$$

In the present study, electrophoretic shaping from ethanolic suspension was investigated to obtain a homogenous Al_2O_3 green body with high density. The stability of Al_2O_3 suspensions was evaluated in ethanol in terms of electrophoretic mobility, viscosity and conductivity. The kinetics of EPD was studied, to clarify the evolution of voltage and deposition time with different experimental conditions. Presintering and HIPing were employed to sinter the Al_2O_3 green body, shaped by EPD.

2. Experimental

The powder used is commercially available TM-DAR α-Al_2O_3 powder (Boehringer Ingelheim Chemicals, Tokyo, Japan), with a purity of 99.99%, an average particle size of 150 nm (d_{50}) and a BET surface of 14.69 m^2/g. Ethanol (purity 99.6 vol.%) without further purification is used as the dispersing medium. The dispersant used is polyethylene imine (PEI, Sigma-Aldrich Company, U.S.), a ''universal'' additive for the EPD of metallic and ceramic powders [9]. Its unit formula of $–[CH_2–CH_2–NH]_n–$ indicates the functional amine –NH groups, which readily adsorb protons in the suspension. PEI becomes charged positively, according to the following reaction [21]:

$$-[CH_2-CH_2-NH]_n + nH^+ \rightleftharpoons -[CH_2-CH_2-NH_2^+]_n$$

The suspensions with different solids loadings (20–70 wt%) were prepared with 0.5–2 wt% PEI by ball milling for 1 h. The resultant suspensions were checked in terms of electrophoretic mobility (Zetaplus, Brookhaven Instruments Co., U.S.), viscosity (Rheomat Mettler SR5) and conductivity (Cyberscan PC510, U.S.) to determine the optimal dispersing conditions. Suspension pH was adjusted with glacial acetic acid (HAc) and tetramethyl ammonium hydroxide (TMAH).

pH was measured with a pH meter (Leici PHSj-4a, China) at room temperature (25.0 °C ± 0.5 °C). Three aqueous standards of pH 4, 7 and 11 were used for standardization due to the lack of standard buffer solutions for ethanol. Thus, the pH meter determines so-called ''operational pH values'' (O.pH) for non-aqueous suspensions. The theoretical background and method involving O.pH was described by Wang et al. [20]. They explained that in any medium the O.pH differs from the actual pH (pa_H) by the residual liquid-junction potential, ΔE_j

$$\mathrm{pH} - pa_H = \frac{\Delta E_j}{0.05916} \quad (\text{at } 25\,^\circ\mathrm{C}) \tag{1}$$

where pH is the pH meter reading, and pa_H (=$-\log a_H$) is the negative logarithm of the proton activity in a non-aqueous suspension. The ΔE_j is the residual liquid-junction potential encountered in the standardization and testing step of a standard

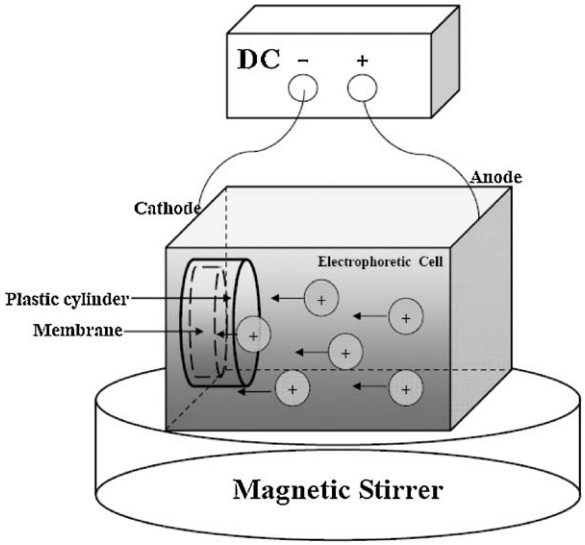

Fig. 1. Schematic diagram of electrophoretic deposition cell.

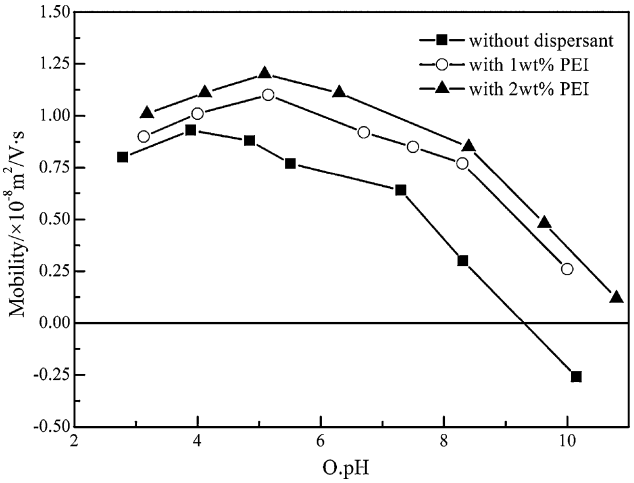

Fig. 2. Electrophoretic mobility of Al_2O_3 with and without PEI addition in ethanol.

pH meter. For the ethanol suspension, $(\Delta E_j/0.05916) = -1.23$ as calculated by Wang et al. [20]. In this paper, the uncorrected O.pH was used for convenience.

A simple experimental setup for EPD is shown in Fig. 1. The distance between two electrodes was usually adjusted to 20 mm. A plastic cylinder with an inner diameter of 25 mm was fixed to the cathode, which was used as a ''mould'' to obtain green body with sharp edges. To easily separate the green body and the electrode, the cellulose acetate membrane was placed between the electrode and the cylinder. The suspensions were stirred with a magnetic stirrer at a low speed to avoid turbulence during the deposition process. The EPD experiments were performed using a power supplier (KIKUSUI, PAN150-2.5A, Japan) which can operate at both constant voltage and constant current density. The shaped green bodies were easily removed from the membrane. After dried in ambient humidity for 24 h, the green bodies were thermally treated at 800 °C for 2 h in air to remove the organic additives and then pressurelessly sintered at 1250 °C for 2 h in air. Finally, they were HIPed at 180 MPa under argon at 1250 °C for 2 h.

The thickness of the green body was determined with a Digimatic Indicator. The green density was determined following the Archimedes principle. Pore size of the green body was obtained by the mercury immersion method. FESEM (JSE-6700F, JEOL, Japan) and SEM (JEOL EPMA8100, Japan) was used to observe the microstructure of green body and sintered alumina. The average grain size was determined from the average linear intercept length multiplied by 1.56 from SEM images of the samples [22].

3. Results and discussion

3.1. Suspension stability

Fig. 2 shows the electrophoretic mobility versus O.pH of Al_2O_3 suspensions with various amounts of PEI. In the absence of PEI, the isoelectric point (IEP) of Al_2O_3 was measured at O.pH 9.3. A maximum electrophoretic mobility was achieved at O.pH 4, and the mobility decreased up to the IEP and then became negative with further increasing O.pH. The adsorption of the positively charged PEI on the surface of Al_2O_3 particles not only significantly shifted the IEP to a higher O.pH value, but also increased the mobility at a given O.pH value. And a maximum mobility was reached at O.pH 5 for the addition of PEI.

In the absence of PEI or a small amount (<0.5 wt%) of PEI, the stability of the suspensions with high solid loadings of >30 wt% could not be retained during the process of EPD, because of the considerable sedimentation. These low-stability suspensions were neglected in further calculations. Fig. 3 shows the variation of the apparent viscosity as a function of O.pH value at a shear rate of 500 s^{-1} with 50 wt% solid loading. As the O.pH decreased, the viscosity increased, indicating a destabilization. This is due to the protonation of PEI. As the O.pH decreases, the number of positively charged sites of PEI continually increases. Under this condition, the branched chains of the positively charged PEI tend to repel each other,

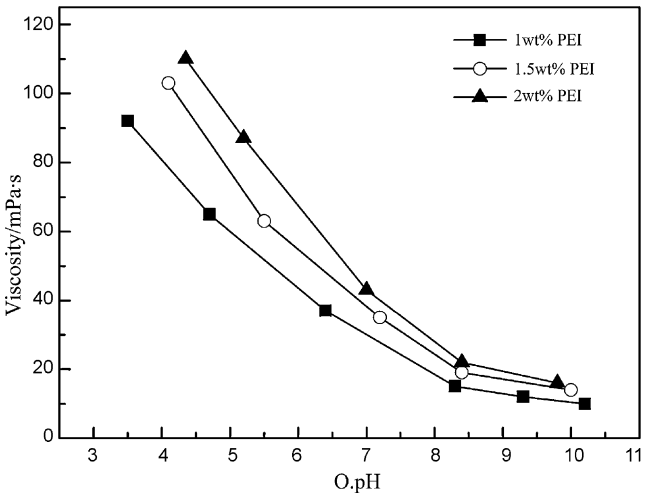

Fig. 3. Viscosities of Al_2O_3 suspensions versus O.pH, at different PEI amounts, at a shear rate of 500 s^{-1} (solid loading: 50 wt%).

and the molecules are in the form of relatively large and expanded stretched chains. Consequently, the surface area per adsorbed chains is relatively high, and less PEI is required to establish a saturated monolayer [23]. Therefore, the reason for destabilization was possibly due to the flocculation induced by the excess non-adsorbed PEI molecules [24–26], which accumulated with the decreasing O.pH. Also, it was clear that the viscosity generally increased with the increasing PEI amount at a given O.pH, which was in good agreement with the increasing free PEI concentration. However, the minimum viscosity near the IEP was associated with a relatively low electrophoretic mobility. Note that the suspensions with 1–2 wt% PEI showed the initial O.pH value ~8.4, where the corresponding mobility was relatively high and the viscosity remained at a low level. Stable suspension with 1 wt% PEI in the initial state was considered to be suitable for EPD.

Another important parameter to be considered is the electrical conductivity. For non-aqueous medium, a low electrical conductivity is necessary to reduce the Joule heating to retain the stability of suspension in the processing of EPD. The conductivity versus solid loading of Al_2O_3 suspensions is shown in Fig. 4. The conductivity increased remarkably with increasing solid loadings. When the solid loading was 70 wt%, the conductivity reached 45 μs cm^{-1}. However, such a high solid loading resulted in a high viscosity of 90 mPa s at a shear rate of 500 s^{-1}, which was inappropriate for EPD. Thus the solid loading of suspension should be below 70 wt%.

3.2. Electrophoretic deposition

3.2.1. The influence of membrane

According to Moritz et al. [27], the adhesion between the green body and the electrode should be minimal so that they can be easily separated. In the present work, a semi-permeable cellulose acetate membrane was stuck on the electrode to prevent the particles to directly deposit on the electrode. To clarify the influence of the membrane, two experiments with and without membranes were performed with the same suspension (50 wt% solid loading and 1 wt% PEI) under a constant voltage of 80 V for 5 min. As summarized in Table 1, the thickness, relative density and weight per unit area of the green body deposited on the membrane were slightly lower than those of the green body done without the membrane. This was due to the semi-permeable membrane just as a resistance, not involving in the deposition mechanism, which demonstrated that the current is mainly carried by ions. Furthermore, the membrane made it easy to remove green body.

Table 1
Green density, thickness and weight per unit area of the deposits obtained from a suspension of 50 wt% Al_2O_3 by applying 80 V for 5 min.

Green deposit characteristics	Membrane	Electrode
Thickness (mm)	2.09	2.15
Relative density (%TD)	59.9	60.1
Weight per unit area (mg/cm^2)	500	513

3.2.2. Kinetics of EPD

Fig. 5 shows the deposited mass per unit area as a function of deposition time and applied voltage for the suspension with the solid loading of 50 wt%. Obviously, under each applied voltage, the increasing deposit time brought an increasing weight per area up to a maximum, 740 mg/cm^2. And the time for the maximum deposit decreased remarkably from 25 min to 5 min with increasing applied voltage from 50 V to 200 V. Take the applied voltage of 100 V for example, after the maximal weight per area has been reached at 20 min, the increment of deposited weight related to the increment of deposit time (another 5 min) became zero since the exhaustion of suspension zone, which transformed into supernatant zone in the process of EPD, with a significantly lower conductivity caused by a decreased concentration of ionic species, where EPD did not continue [12]. In general, the weight per area and the deposit time should be in accordance with the following equation from

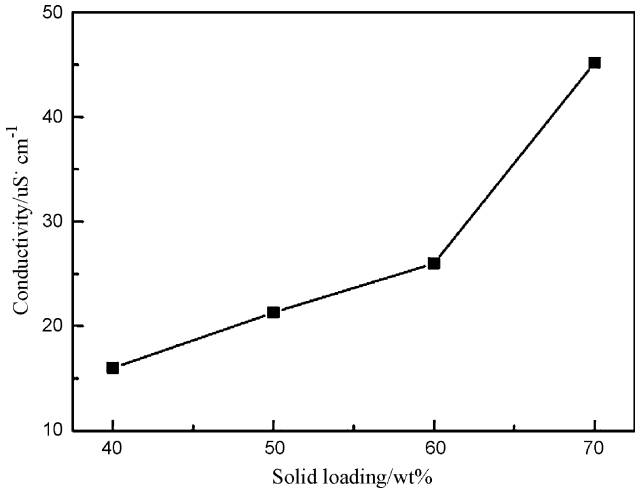

Fig. 4. Variation of the conductivity with solid loadings (dispersant concentration: 1 wt% PEI).

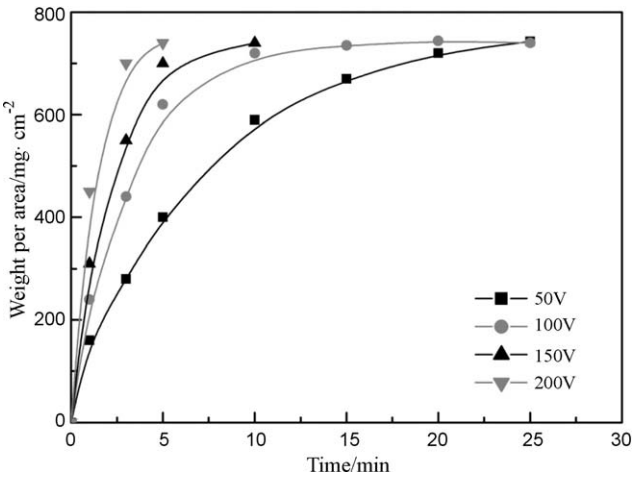

Fig. 5. Weight per area as a function of deposition time under different applied voltages.

Hamaker's equation [28]:

$$w = \rho d = \frac{2}{3} C \varepsilon_0 \varepsilon_\Gamma \xi \left(\frac{1}{\eta}\right)\left(\frac{E}{L}\right) t \quad (2)$$

where w is the weight of charged Al_2O_3 deposited per unit area, ρ is the green density, d is the thickness of green body, C is the solid loading of suspension, ε_0 is the permittivity of vacuum, ε_Γ is the permittivity of the solvent, ξ is the zeta potential of the particles, η is the viscosity of suspension, E is the applied potential, L is the distance between the electrodes and t is the deposit time. However, in contrast to the linear prediction of weight per area with time from Eq. (2), a non-linear increase in deposit occurred right after start of the experiment. Such deviation from linearity is possible in a constant voltage EPD because of several factors. The most commonly attributed factor is that due to the effect of the electrically resistive deposition [29]. Apparently the current decreased with time because of the aforementioned reasons, and vanished at the time when the maximum deposit realized, which was used to judge whether EPD should be stopped in the present study. As mentioned above, a higher voltage applied would achieve the maximal weight per area in a shorter time, which was favorable to retain the stability of suspension. However, a rough surface would happen when the voltage of >100 V was applied. This may possibly be because of the high deposition rates at higher applied voltages at which the particles do not get sufficient time to sit at closest possible packing positions before deposition of incoming particles. Therefore, the applied voltage of 100 V was the optimal condition for the present experiments.

3.2.3. Effect of solid loading

Solid loading is usually considered not to affect EPD, except for the fact that the higher the quantity of solids in the suspension was, the higher the quantity of particles deposited. To clarify this point, the experiments were performed under the same deposition conditions (applied voltage: 100 V and deposit time: 10 min). The results are plotted in Fig. 6. The green density was normally around 60 %TD, consistent with values of non-conducting powders reported in the literature [30], which indicated that the particles were closely packed in the deposit after drying. And the increase in the thickness of deposition and with increasing solid loading of suspension was linear and in accordance with Eq. (2). Therefore, the present experimental results demonstrated that the solid loading could be a powerful tool to obtain the required thickness. Considering the stability of suspension and deposit thickness, the solid loading should be in the range 50–60 wt%.

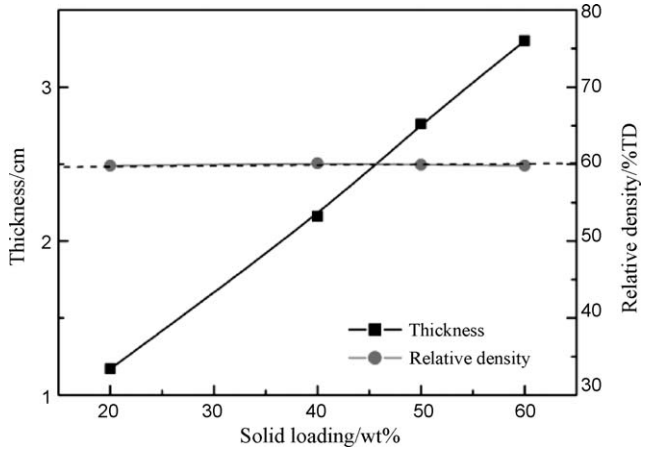

Fig. 6. Thickness and relative density as a function of solid loading (applied voltage: 100 V and deposit time: 10 min).

3.3. Microstructure

The cross-section microstructure of the green body is shown in Fig. 7. No cracks were found under FESEM. To illustrate the degree of homogeneity of particle coordination in the present investigation, Fig. 8 compares the pore size distributions of green bodies prepared by EPD and other shaping methods described in Ref. [7], which used the same TM-DAR powder. In Fig. 8, relative pore size distributions were provided with the curves running from 0 to 100 relative percents independent of the total absolute porosities that were quoted as a parameter. According to Krell and Klimke [7], the similar slope of the pore

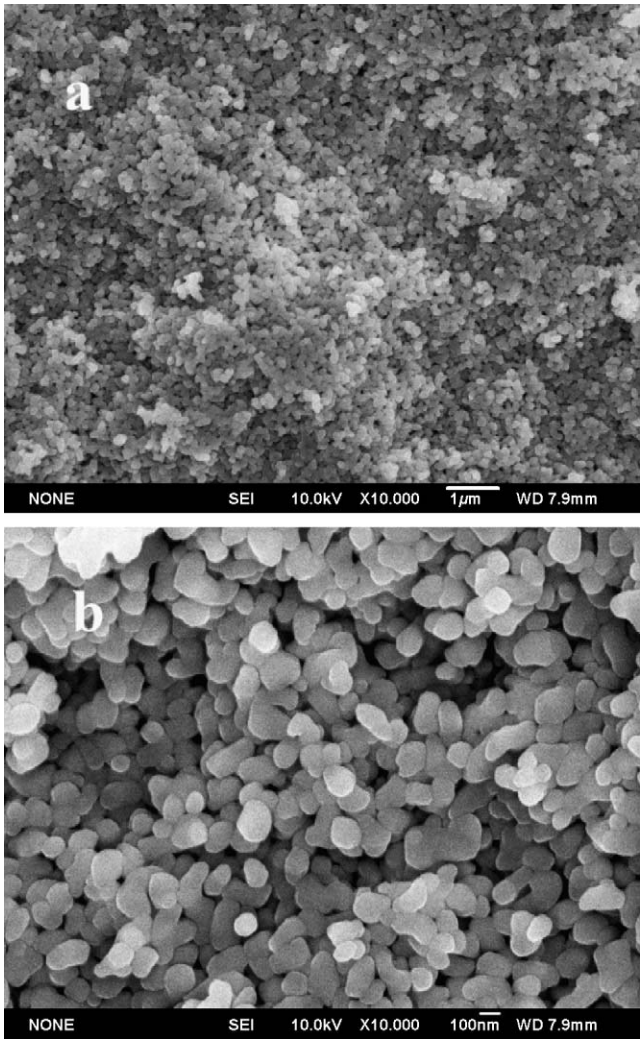

Fig. 7. FESEM photographs of the fracture surface of EPD deposit (a) EPD deposit and (b) magnification of (a).

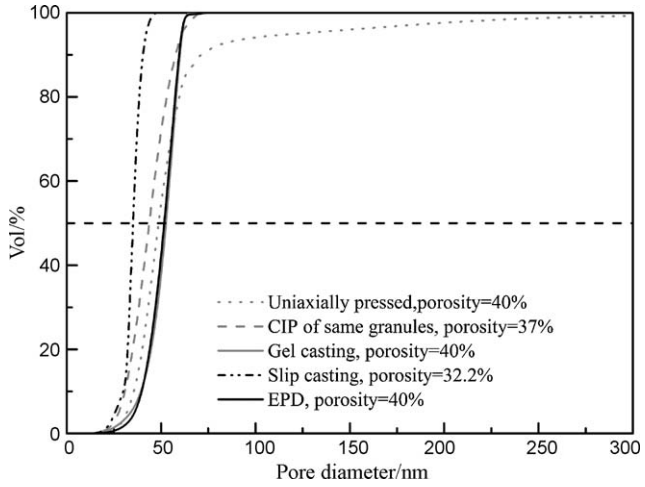

Fig. 8. Pore size distribution of Al_2O_3 samples manufactured from TM-DAR powder by (i) uniaxially pressing, (ii) CIPing, (iii) gel casting, (iv) slip casting and (v) EPD (after heated to 800 °C).

size distribution gave evidence of a similar homogeneity. Apparently, the pore size distribution of EPD was the same as gel casting, indicating an identical homogeneity of particle coordination could be achieved in EPD as in gel casting. Slip casting exhibited a similar homogeneity as gel casting due to the similar slope of pore size distribution, while uniaxially pressing and CIPing showed a poor homogeneity because of their wider distributions. Therefore, EPD could provide the microstructural reason of the successful low-temperature sintering of ultrafine powders.

After presintered at 1250 °C, relative density of the sample, shaped by EPD, reached 95.3 %TD, with an average grain size of 0.6 μm (Fig. 9), which was sufficient for further treatment by HIP. Fig. 10 shows the dense alumina ceramic (thickness of 1 mm), with an average grain size of 0.65 μm after HIPed at 1250 °C for 2 h. And a similar grain size of 0.66 μm was reported in the case of gel casting under the same sintering conditions [3]. It was also suggested that electrophoretic deposition woule be an appropriate approach to prepare polycrystalline alumina ceramic with sub-microstructure, like gel casting.

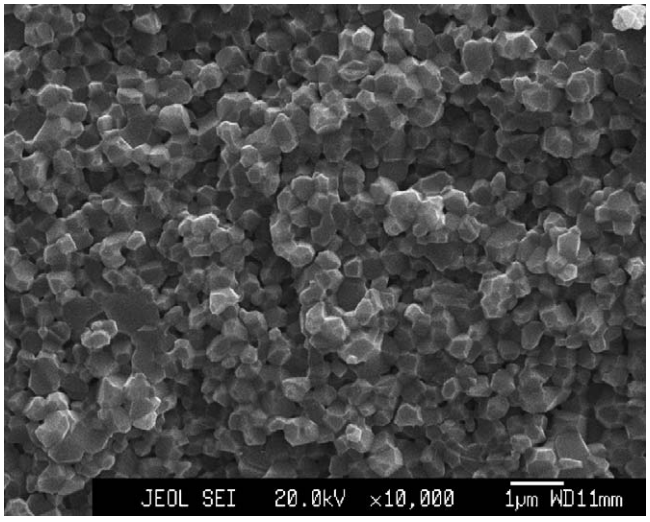

Fig. 9. Fracture surface of sub-micron alumina by EPD after presintered at 1250 °C.

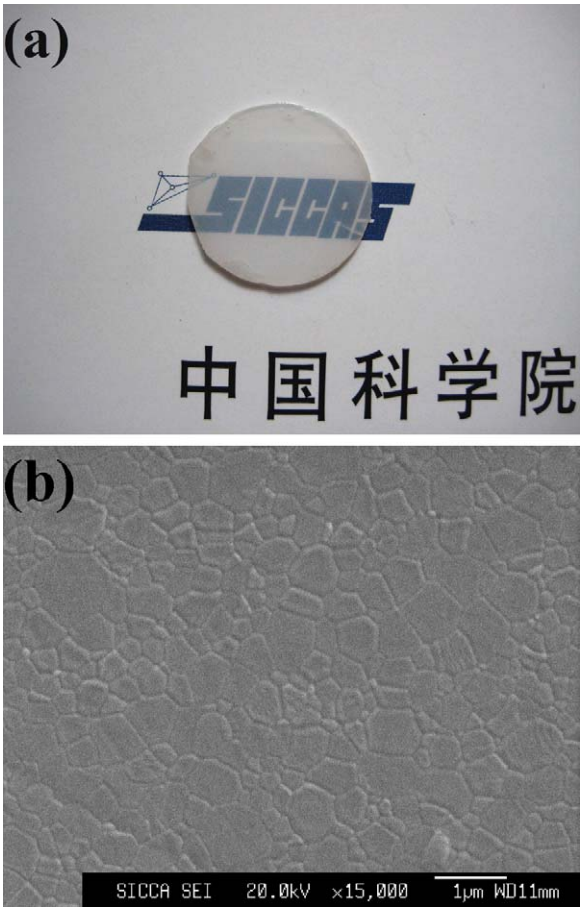

Fig. 10. (a) Fully dense polycrystalline Al_2O_3 (1 mm thickness) and (b) SEM image of it.

4. Conclusions

The uniform and high green density deposit of ultrafine Al_2O_3 by EPD in ethanol suspension has been reached. The stable suspensions with 50–60 wt% solid loadings were prepared by adding 1 wt% PEI as dispersant, which is an important prerequisite for a successful EPD. With increasing applied voltage or deposit time, weight per area increased until the maximum deposit resulted. The density of green body obtained under the optimal conditions was 60.4 %TD. SEM and pore size distribution reflected a homogeneous particle packing in the green body, similar with gel casting. After presintering and HIPing at 1250 °C, a fully dense alumina ceramic with an average grain size of 0.65 μm was successfully obtained. The result shows that electrophoretic deposition is a promising way to obtain polycrystalline alumina ceramic with sub-microstructure.

References

[1] C. Scott, M. Kaliszewski, C. Greskovich, L. Leonson, Conversion of polycrystalline Al_2O_3 into single-crystal sapphire by abnormal grain growth, J. Am. Ceram. Soc. 85 (5) (2002) 1275–1280.

[2] G.C. Wei, A. Hecker, D.A. Goodman, Translucent polycrystalline alumina with improved resistance to sodium attack, J. Am. Ceram. Soc. 84 (12) (2001) 2853–2862.
[3] A. Krell, P. Blank, H. Ma, T. Hutzler, M.P.B. van Bruggen, R. Apetz, Transparent sintered corundum with high hardness and strength, J. Am. Ceram. Soc. 86 (1) (2003) 12–18.
[4] A. Krell, S. Schadlich, Nanoindentation hardness of submicrometer alumina ceramics, Mater. Sci. Eng. A 307 (1/2) (2001) 172–181.
[5] A. Krell, P. Blank, H. Ma, T. Hutzler, Processing of high-density sub-micrometer Al_2O_3 for new applications, J. Am. Ceram. Soc. 86 (4) (2003) 546–553.
[6] A. Krell, H.-W. Ma, Sintering transparent and other sub-μm alumina: the right powder, *cfi*, Ber. Dt. Keram. Ges. 80 (4) (2003) E41–E45.
[7] A. Krell, J. Klimke, Effects of the homogeneity of particle coordination on solid-state sintering of transparent alumina, J. Am. Ceram. Soc. 89 (6) (2006) 1985–1992.
[8] A. Krell, B. Blank, The influence of shaping method on the grain size dependence of strength, J. Eur. Ceram. Soc. 16 (11) (1996) 1189–2000.
[9] Y. Fukada, N. Nagarajan, W. Mekky, Y. Bao, Electrophoretic deposition-mechanisms, myths and materials, J. Mater. Sci. 39 (2004) 787–801.
[10] F. Harbach, H. Nienburg, Homogeneous functional ceramic components through electrophoretic deposition from stable colloidal suspensions. I. Basic concepts and application to zirconia, J. Eur. Ceram. Soc. 18 (6) (1998) 675–683.
[11] F. Bouyer, A. Foissy, Electrophoretic deposition of silicon carbide, J. Am. Ceram. Soc. 82 (8) (1999) 2001–2010.
[12] K. Moritz, E. Muller, Investigation of the electrophoretic deposition behaviour of non-aqueous ceramic suspensions, J. Mater. Sci. 41 (2006) 8047–8058.
[13] J. Tabellion, R. Clasen, Electrophoretic deposition from aqueous suspensions for near-shape manufacturing of advanced ceramics and glasses—applications, J. Mater. Sci. 39 (2004) 803–811.
[14] A.V. Kerkar, R.W. Rice, R.M. Spotnitz, U.S. Patent No. 5,194,129.
[15] T. Uchikoshi, K. Ozawa, B.D. Hatton, Y. Sakka, Dense, bubble-free, ceramic deposits from aqueous suspensions by electrophoretic deposition, J. Mater. Res. 16 (2) (2001) 321–324.
[16] C.H. Oetzel, R. Clasen, J. Tabellion, Electric-field assisted processing of ceramics, Ceram. Forum Int. 81 (4) (2004) E35–E41.
[17] A. Braun, G. Falk, R. Clasen, Transparent polycrystalline alumina ceramic with sub-micrometre microstructure by means of electrophoretic deposition, Mater. Wiss. Werkst. 37 (4) (2006) 293–297.
[18] O. Van der Biest, L.J. Vandeperre, Electrophoretic deposition of materials, Annu. Rev. Mater. Sci. 29 (1999) 327–352.
[19] J. Lyklema, Principles of the stability of lyophobic colloidal dispersions in non-aqueous media, Adv. Colloid Interf. Sci. 2 (1968) 65–114.
[20] G.-H. Wang, P. Sarkar, P.S. Nicholson, Influence of acidity on the electrostatic stability of alumina suspensions in ethanol, J. Am. Ceram. Soc. 80 (4) (1997) 965–972.
[21] F.Q. Tang, X.X. Huang, Y.F. Zhang, J.K. Guo, Effect of dispersants on surface chemical properties of nano-zirconia suspensions, Ceram. Int. 26 (1) (2000) 93–99.
[22] M.I. Mendelson, Average grain size in polycrystalline ceramics, J. Am. Ceram. Soc. 52 (8) (1969) 443–446.
[23] G.M. Lindquist, R.A. Stratton, The role of polyelectrolyte charge density and molecular weight on the adsorption of colloidal silica with polyethylenimine, J. Colloid Int. Sci. 55 (1976) 45–59.
[24] T. Uchikoshi, T. Hisashige, Y. Sakka, Stabilization of yttria aqueous suspension with polythylenimine and electrophoretic deposition, J. Ceram. Soc. Jpn. 110 (9) (2002) 840–843.
[25] X. Zhu, T. Uchikoshi, Z. Suzuki, Y. Saaka, Effect of polyethylenimine on hydrolysis and dispersion properties of aqueous Si_3N_4 suspensions, J. Am. Ceram. Soc. 90 (3) (2007) 797–804.
[26] J. Cesarano III, I.A. Aksay, Processing of highly concentrated aqueous α-alumina suspensions stabilized with polyelectrolyte, J. Am. Ceram. Soc. 71 (12) (1988) 1062–1067.
[27] T. Moritz, W. Eiselt, K. Moritz, Electrophoretic deposition applied to ceramic dental crowns and bridges, J. Mater. Sci. 41 (2006) 8123–8129.
[28] P.M. Biesheuvel, H. Verweij, Calculation of the composition profile of a functionally graded material produced by centrifugal casting, J. Am. Ceram. Soc. 83 (4) (2000) 743–749.
[29] G. Anne, B. Neirinck, K. Vanmeensel, O. Van der Biest, J. Vleugels, Origin of the potential drop over the deposit during electrophoretic deposition, J. Am. Ceram. Soc. 89 (3) (2006) 823–828.
[30] M.S.J. Gani, Electrophoretic deposition: a review, Ind. Ceram. 14 (1994) 163–174.